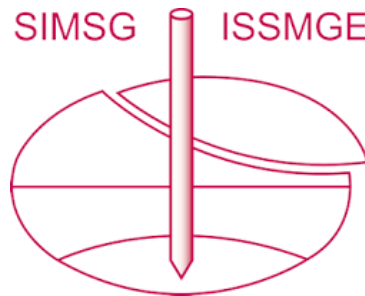


INTERNATIONAL SOCIETY FOR SOIL MECHANICS AND GEOTECHNICAL ENGINEERING



This paper was downloaded from the Online Library of the International Society for Soil Mechanics and Geotechnical Engineering (ISSMGE). The library is available here:

<https://www.issmge.org/publications/online-library>

This is an open-access database that archives thousands of papers published under the Auspices of the ISSMGE and maintained by the Innovation and Development Committee of ISSMGE.

The paper was published in the proceedings of the 7th International Conference on Earthquake Geotechnical Engineering and was edited by Francesco Silvestri, Nicola Moraci and Susanna Antonielli. The conference was held in Rome, Italy, 17 - 20 June 2019.

Special Lectures

Ishihara Lecture



Taylor & Francis

Taylor & Francis Group

<http://taylorandfrancis.com>

Summarizing geotechnical activities after the 2011 Tohoku earthquake of Japan

I. Towhata

Kanto Gakuin University, Yokohama, Japan

ABSTRACT: After the 2011 Tohoku earthquake in Japan, I as the Vice President and then as the President of the Japanese Geotechnical Society took initiatives in damage reconnaissance, developing new safety criterion for liquefaction-prone residential areas, quantitative evaluation of ageing effects on liquefaction resistance of sand, investigation on damage mechanism of river levees, recovery from the tsunami incidence of Fukushima No.1 Nuclear Power Plant and ground improvement in existing residential area. Some of them were conducted urgently within several months after the earthquake, while others encountered many difficulties from the viewpoint of public agreement. This paper summarizes the post-earthquake activities of geotechnical engineering in restoration of the community.

1 INTRODUCTION

The 2011 Tohoku earthquake of Japan registered the seismic magnitude of $M_w=9.0$. This event forced people to change their idea on safety during natural disasters. Before this earthquake, people demanded engineers to achieve zero risk during natural disasters and engineers believed that it is possible. After this earthquake, in contrast, people understood that zero risk is impossible under such a rare event. Nevertheless, it appears that they are not yet prepared reasonably for possible extreme events. They are either unnecessarily scared by the worst but rare event or still overlook the risk of natural disasters. This paper addresses the experience of the author who had opportunities after the 2011 earthquake to be involved in a variety of post-disaster activities that were related with geotechnical engineering.

2 SEISMOLOGICAL ASPECTS OF THE 2011 TOHOKU EARTHQUAKE

The Pacific Coast of Eastern Japan (Figure 1) is a seismically active region. Because of the subduction of the Pacific Ocean Plate, many gigantic earthquakes occurred there in the past and some of them triggered disastrous tsunamis. Noteworthy is that those earthquakes and tsunamis in the past occurred in the northern part of Tohoku coast (Figure 1) and that much was not known about the seismic vulnerability in the southern part (HERP, 2009). This lack of knowledge became important later in the context of safety of nuclear power plants in the southern coast. Figure 2 shows the historical earthquake disasters in the Pacific Coast of Tohoku. They occurred in the Sendai City area and in the northern part of the Pacific coast. Obviously many gigantic earthquakes occurred in this region and tsunami disasters were repeated. The problem is the lack of earthquake and tsunami information from 9th to 16th Century. Because the Tohoku Region was far from the capital (Kyoto), written record was not preserved of natural disasters. Even the official record on the AD 869 earthquake had not been fully trusted because of its unclear description.

Based on the repetition of gigantic earthquakes in the past, the next big one had been expected for decades. Figure 3 illustrates the occurrence of many earthquakes in the Pacific Coast area of Tohoku and its surroundings before and after the 2011 main shock. When the one on March 9 (two days before the catastrophic one) registered $M=7.3$ off Sendai, it was thought that the expected one occurred. It was unfortunately wrong and most probably this event was a foreshock.



Figure 1. Tohoku Region and Sendai.

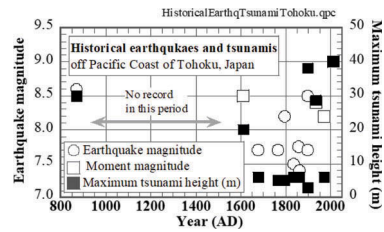


Figure 2. History of earthquakes in Pacific Coast Region of Tohoku, Japan (Northern Tohoku) (Most data after Hatori, 1975).

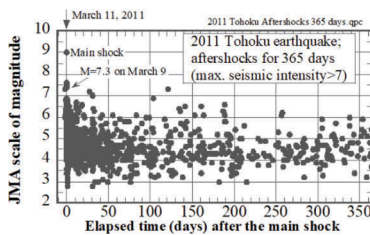


Figure 3. Aftershocks in Tohoku Region (data by Japan. maximum seismic intensity>3).

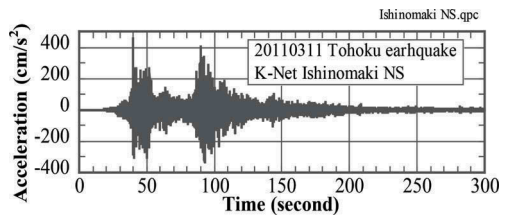


Figure 4. K-Net acceleration record of Tohoku Meteorological Agency; earthquake at Ishinomaki (NS component).

The earthquake of Mw=9 in 2011 was triggered by tectonic rupture off the entire Pacific Coast of the Tohoku Region. The size of rupture was 500 km in NS direction and 200 km in EW direction (JMA, 2011), thus generating tsunami wave over the entire coast of Tohoku. Figure 4 illustrates the time history of acceleration that was recorded by K-Net Ishinomaki Station which is near Sendai. This shaking is characterized by its long duration of the strong phase, consisting of many number of cycles, and two particularly strong phases of shaking at around 50 and 100 seconds, respectively. The latter feature was produced by two separate ruptures in the earth crust. The Tohoku earthquake was generated by consecutive rupture of many crustal pieces.

Aftershocks continued for months. Figure 3 suggests that the number of events came back to the original (background) level about 200 days after the main shock. During the aftershock period, there was a rumor that another catastrophic quake was coming to Tokyo Region. In such a situation, it was difficult to initiate a reconstruction plan of the community except emergency activities.

3 GEOTECHNICAL DAMAGE

Because many reports have been published on damage, this chapter introduces only typical ones that facilitate the readers' understanding of the following chapters.

3.1 Tsunami

It is obvious that tsunami on March 11th was the major cause of catastrophic damage. Its height exceeded the previous expectation and overtopped many sea walls. The tsunami came several times (Figure 5). It appears that the first tsunami destroyed sea walls at many places and there was no safety measure during the following tsunami attacks. Note that the sea level did not retreat prior to the first tsunami, contradictory to what some people believe. The sea wall in Figure 6 was damaged by in-flow of water that scoured the toe on its land side. After loss of lateral support in its foundation, the sea wall was easily transported landwards by later in-coming tsunami. This appears different from the experience in Banda Aceh where harbor structures moved seawards.

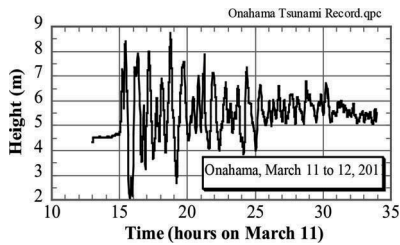


Figure 5. Sea level change in Onahama Harbor during the tsunami attack on March 11, 2011 (after Japanese Meteorological Agency).



Figure 6. Damaged seawall near the Abukuma River mouth.



Figure 7. Destroyed community behind seawall (Tohni-Hongo).



Figure 8. Rikuzen-Takata after tsunami washing.

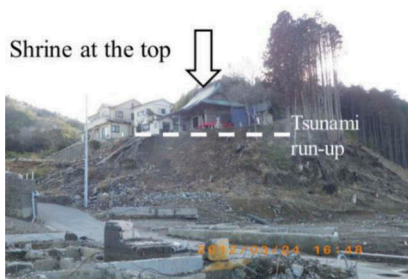


Figure 9. Shrine atop a slope in Onagawa where where tsunami stopped in its front.



Figure 10. Shrine in Ohzuchi at very low elevation tsunami stopped in its front.

Figure 7 shows the situation in Tohni-Hongo where the local community had been relocated to higher places after the previous tsunami in 1933. Thereafter, a sea wall was constructed; its height was higher than the tsunami in 1933. As a consequence, people felt safe and many of them came back to the coastal area. This was a reasonable decision because most people lived on fishing. In 2011, the tsunami was higher than the wall and the community behind the wall was totally destroyed. This is an unfortunate evidence to show that empiricism (height of previous tsunami) is not fully reliable under rare catastrophic natural disasters. Overtopping occurred in many other towns as well (Figure 8).

The risk of catastrophic but rare disaster may be more reasonably assessed by non-engineering studies. Along the Pacific Coast of Tohoku region, there are many shrines (temples of Japanese gods). It is likely that those shrines were destroyed by past tsunamis and that local people reconstructed them at safer (higher) places. Consequently, the tsunami run-up in 2011 stopped in front of the shrine at many places (Uda et al., 2012; Matsuura, 2013). Figure 9 is

one of the examples for this. Since the tsunami height varies with the submarine topography (bathymetry), it was very low at some places. Figure 10 is an example of such a place where the shrine at low elevation survived the disaster. These facts imply the importance of historical knowledge that may not appear scientific from the modern technological viewpoints. Note, however, that Yamazaki (2013) together with Endo and Mazereeuw (2015) attributes the shrine location to other historical/political and cultural reasons.

3.2 *Coseismic subsidence due to tectonic action*

It is well known that gigantic earthquakes in the subduction zone are triggered by rebound of continental tectonic plates after rupture in its interface with the ocean plates. The rebound results in the uplift of the sea bed and triggers tsunami. At the same time, the inland part of the continental plate subsides because the rebound-induced elongation in the horizontal direction is associated with vertical contraction; recall *Poisson* ratio. Figure 11 is an example of such coseismic subsidence in Banseki-Ura near Sendai where the ground subsidence exceeded 1m. Similar subsidence occurred during the 1946 Nankai earthquake of $M_w=8.4$ in Japan (Kawasumi and Sato, 1949), the 1960 Chile earthquake of $M_w=9.5$ (Housner, 1963) and the 1964 Alaska earthquake of $M_w=9.2$ (Plafker, 1969). Figure 12 exhibits the post-earthquake situation of Onagawa Nuclear Power Plant that was situated at 14.8 m above the sea level. This height was sufficient to survive the tsunami inundation but the tsunami water came into the power plant through an underground conduit into one of the excavated basement spaces. Fortunately, the water was stopped by a water-tight door at the entrance of the reactor building. Noteworthy is that the power plant site had subsided one meter by the tectonic mechanism, without which the plant would have been safer.

The tectonic subsidence together with the loss of sea wall due to tsunami caused fear of safety against high sea wave during the typhoon season of 2011. It was fortunate that no typhoon came to the Tohoku region in that year. Figure 13 shows the time history of recovery of ground level after the earthquake. More profound subsidence occurred in the central part of Tohoku region (Miyako, Taro, Miyagi Yamoto, Onagawa and then Iwaki), while less subsidence occurred at far places. It is interesting that the rate of recovery is very slow in contrast to the experience after the 1946 Nankai earthquake after which the ground level recovered substantially within half year (Sect. 16.10 in Towhata, 2008).

3.3 *Subsoil liquefaction*

Japanese Geotechnical Society and the Kanto Regional Development Bureau of the Ministry of Land, Infrastructure, Transportation and Tourism jointly investigated the location of liquefaction in the Kanto Region and the result is shown in Figure 14 in which red dots account for the sites of liquefaction. It is evident that liquefaction occurred in two kinds of geomorphology which are young man-made islands along the coast of Tokyo Bay and abandoned river channels and former lakes along the Tone River and other big rivers.

There are many man-made islands in the Tokyo Bay. They were constructed by dumping either hill sand or dredged sea-bed sand mostly in the second half of the 20th Century. Figure 14 indicates that liquefaction was significant in those islands between Tokyo and Chiba while not much happened in the eastern coast of the Bay (south of Chiba) and between Tokyo and Kanagawa on the western side. One reason for the “good” performance in the eastern coast is the lack of information. Those “good” islands are industrial areas and factories therein do not release “negative” information nowadays. The other reason is that industries had improved soil conditions in their factories after the 1987 Chiba-ken-Toho-oki earthquake when liquefaction was significant in industrial islands (Kotoda and Wakamatsu, 1988). Consequently, liquefaction in 2011 was concentrated in young residential islands. In contrast, liquefaction hardly occurred in aged subsoil regions except young backfill soil of buried pipelines.

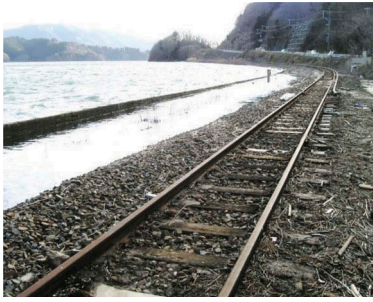
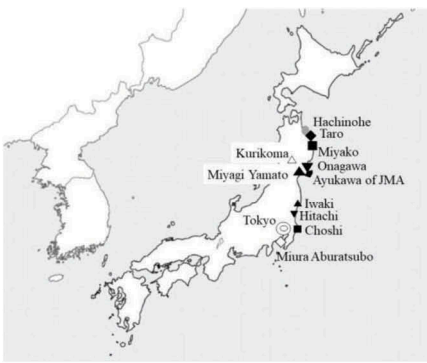


Figure 11. Tectonic subsidence in Banseki-Ura near Sendai.



Figure 12. Onagawa Nuclear Power Plant that marginally survived the tsunami-induced disaster.

(a) Sites of GNSS monitoring



(b) Records of ground level

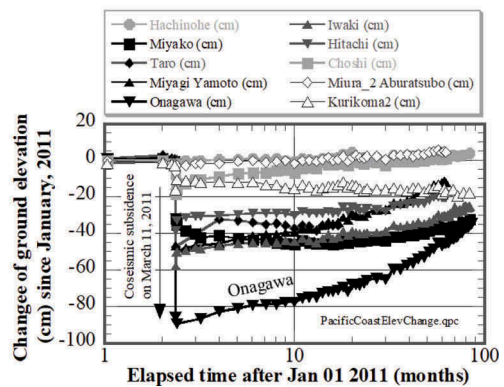


Figure 13. Slow recovery of ground elevation after tectonic subsidence in 2011 (after Earth Observation Network, Geospatial Information Authority of Japan).

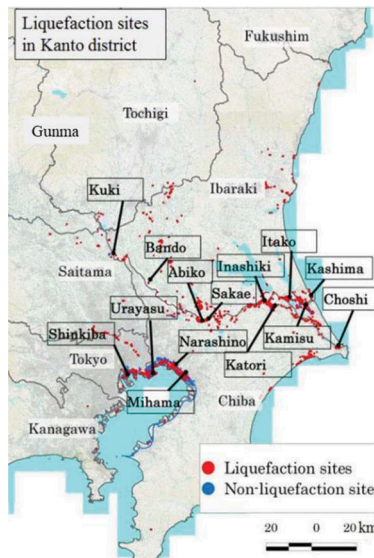


Figure 14. Sites of liquefaction in Kanto Region (Towhata et al., 2014).



Figure 15. Floating of underground parking structure (Yokohama).



Figure 16. Floating of sewage manhole (Itako, Ibaragi).

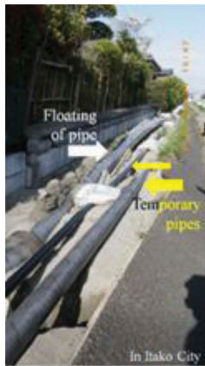


Figure 17. Floating of sewage pipeline in Itako.

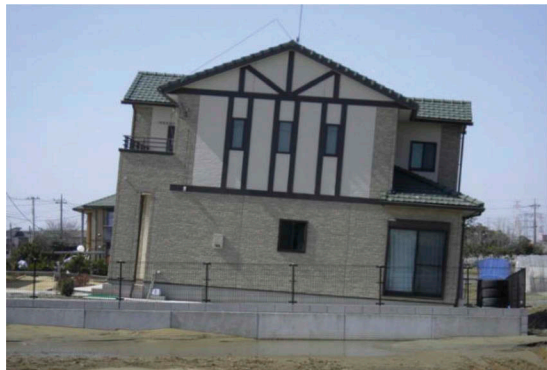


Figure 18. Tilting of house caused by subsoil liquefaction (Kashima, Ibaragi).

(a) Damaged fill part



(b) Intact cut part



Figure 19. Seismic damage of residential land in the suburban hill area of Sendai.

Figure 15 illustrates floating of an underground car parking. Figure 16 shows floating of a manhole and Figure 17 indicates floating of a sewage pipeline. Thus, the vulnerability of sewage lifeline network became evident at many places. Those buried structures that were lighter than unit weight of liquefied sand floated and stopped functions. Tilting of house was repeated as well due to softening of liquefaction-prone subsoil in the foundation. The situation in Figure 18 is the worst and other affected houses exhibited much smaller tilting without structural problem. However, it is nowadays known that tilting of as small as 0.6% causes



Figure 20. Crest subsidence and lateral spreading of Abukuma-River levee (Sasaki et al., 2012).

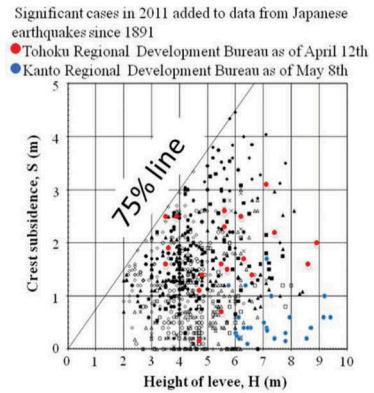


Figure 21. Relation between levee height and subsidence (Sasaki et al., 2012).

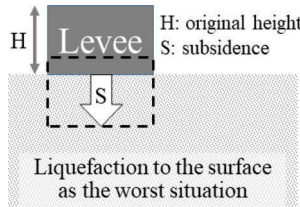


Figure 22. Reason for the maximum crest subsidence not exceeding 75% of the levee height.

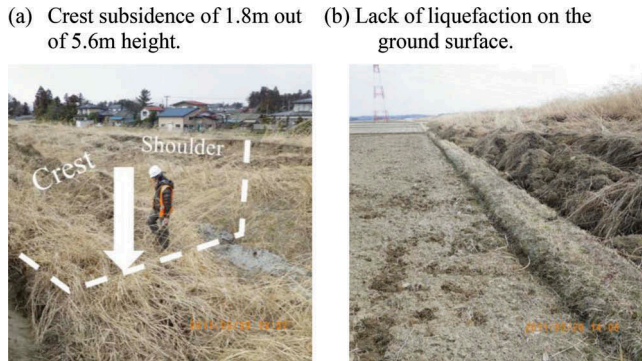


Figure 23. Consequence of liquefaction in levee body (Naruse River, Miyagi Prefecture).

such health problems as headache and dizziness to residents (Kitahara and Uno, 1965; Keino et al., 2011; Kohiyama and Keino, 2012; Kohiyama et al., 2012; Yasuda, 2004).

3.4 Collapse of residential land in hilly area

Sendai area developed its suburban residential land in hilly areas by cutting hills and filling valleys, thus producing level ground. This is in clear contrast with the situation in Kanto Region (Figure 14) where man-made islands were used for new residences. After completion, ground water in hills infiltrated into new fills and increased the weight of soil. Moreover, compaction of fill was insufficient to resist the seismic load and that the shear resistance in the interface between fill and the original valley surface was, most probably, poor. Accordingly, the fill parts collapsed during the earthquake (Figure 19a) and the value of the real estate was lost. Conversely, the cut

part in the vicinity was intact (Figure 19b). The problem is that the ground surface is flat after construction and people cannot capture the original condition (fill or cut) of the land when they purchase it.

3.5 River levee

Significant subsidence occurred in many sections of river levee in both Kanto Plain around Tokyo and Sendai Plain (Figure 1). Figure 20 shows the induced subsidence and lateral spreading. According to the damage summary, the extent of subsidence (S) did not exceed 75% of the original levee height (H) (Figure 21), which is consistent with the previous summary of seismic damage of levees since the 1891 Nobi earthquake of $M=8.0$. The mechanical reason for the upper bound of 75% subsidence is schematically illustrated in Figure 22; compare the unit weight of water-saturated liquefied subsoil (typically 20 kN/m^3) and that of levee with less degree of saturation (typically 15 kN/m^3). Because of the support provided by the bearing capacity of subsoil,

$$\text{Buoyancy } 20(\text{kN/m}^3) \times S(\text{m}) \leq \text{Gravity } 15(\text{kN/m}^3) \times H(\text{m}) \quad (1)$$

The weight of the levee and the buoyancy in its submerged part reach equilibrium at the subsidence (S) equal to 75% of the original levee height (H). 75% subsidence does occur in the worst case in which liquefaction occurs from the ground surface and lasts for a sufficiently long time to allow for the maximum possible extent of ground deformation.

A peculiar mode of levee deformation is shown in Figure 23. At this site, the levee crest subsided significantly, while two shoulders of the slope maintained their original height. Moreover, the local soil condition at the surface in this area is clayey and there is no evidence of liquefaction on the ground surface (Figure 23b). This phenomenon is attributed to liquefaction inside the levee body.

4 ASSESSMENT OF LIQUEFACTION RESISTANCE OF SANDY SUBSOIL

4.1 Ageing of liquefaction resistance of sand

The Tohoku earthquake caused liquefaction so vastly that concern on the validity of existing liquefaction code arose. Ishihara and Sasaki (2012) examined the Highway Bridge Design Code by comparing calculated risk of liquefaction and reality. It was indicated by them that the existing code is reasonable with some safety margin. The margin means that the code slightly underestimates the liquefaction resistance of aged soil. The author believes that this conservatism is important in design of important infrastructures. Noteworthy is that liquefaction risk of private residential land attracted concern at the same time (Figure 18) and people

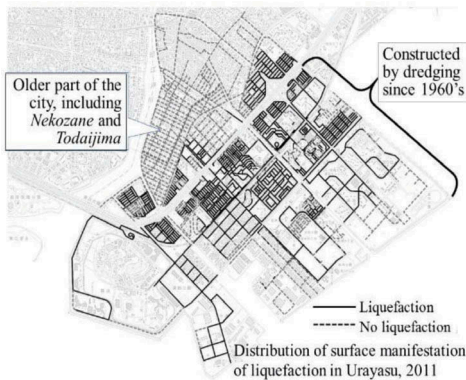


Figure 24. Distribution of liquefaction only in recent man-made island, Urayasu, Chiba.

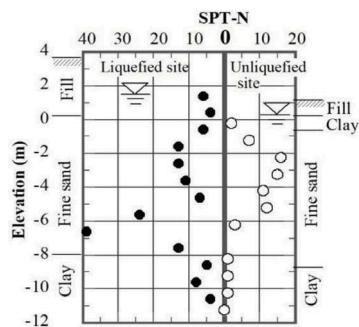


Figure 25. Two similar bore hole profiles at sites with and without liquefaction.

cannot afford conservative ground improvement. In this regard, more precise assessment with less safety margin was desired.

The author paid attention to the age effect on soil. Because of this effect, liquefaction occurred in young man-made islands only (Towhata et al., 2016a). Figure 24 shows the distribution of liquefaction in Urayasu City to the east of Tokyo where onset of liquefaction was limited to very recent man-made islands. Figure 25 compares two similar bore hole logs; one site was located in a man-made island and suffered from liquefaction, while the other in a natural and aged alluvium did not. It was supposed therefore that liquefaction resistance should be assessed by considering the age of soil that is not accounted for in bore hole data.

Tokyo and its surrounding area is an ideal place for study of ageing because locations of liquefaction during the 2011 earthquake are well recorded, many borehole data is available within the area, earthquake motion records are available at many K-Net sites, and the history of land reclamation since the end of 16th Century is known. By using this information together with the formulae of the Highway Bridge Design Code and Recommendations for Design of Building Foundations by AIJ, the factor of safety against liquefaction, F_L , was calculated and compared against

the age of subsoil. The aim was to determine the border factor of safety between liquefaction and no liquefaction which is theoretically equal to 1.0 but may vary with soil age.

The difficulties of the ageing study were as what follows;

1. It is significantly uncertain which soil layer liquefied. Sand ejecta and other surface manifestation of liquefaction do not specify the depth of liquefaction.
2. It is possible that liquefaction occurred at great depth and did not produce surface manifestation.
3. Because the majority of K-NET earthquake monitoring stations are situated on unliquefied sites, no actual ground motion is known at liquefied sites.
4. Sites of K-NET stations and those of analyzed borehole data are not necessarily identical. The F_L values have to be calculated by using the nearest available K-NET motion data.
5. Alluvial deposits are generally assumed to be older than reclaimed manmade islands. However, in the extreme case, soil deposited in the very recent past.
6. Reported liquefaction may be the event in recent backfill of lifelines within older natural deposits.

These difficulties were solved as described in detail in Towhata et al. (2016a) and this paper introduces the most important idea to solve the above-mentioned uncertainty (1). At sites where surface manifestation of liquefaction was reported (Figure 26a), the factor of safety was calculated in the vertical direction and the minimum factor of safety, F_{Lmin} , was determined. The border value is greater than F_{Lmin} because, otherwise, the factor of safety would be greater than the border value throughout the depth and no liquefaction would have occurred. This is obviously against the liquefaction report. Thus, F_{Lmin} is the lower bound. At sites without report of liquefaction (Figure 26b), on the contrary, the maximum value in the F_L profile is taken and considered

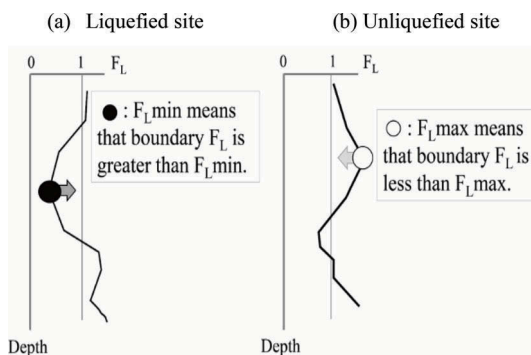


Figure 26. Idea of lower and upper bound of border factor of safety.

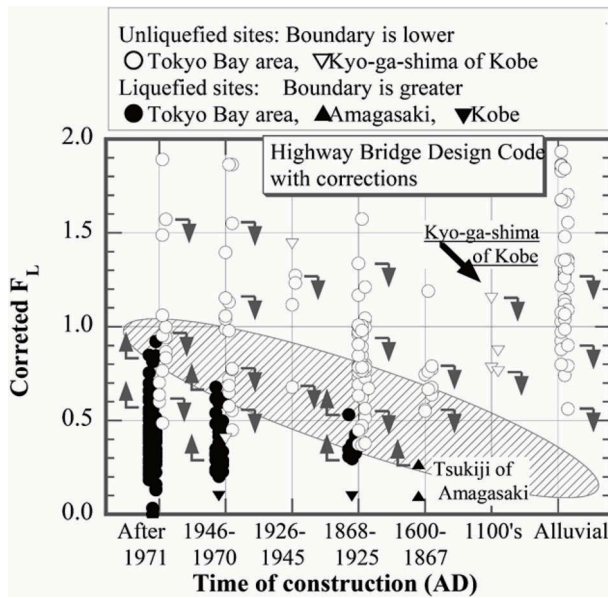


Figure 27. Temporal variation of border factor of safety between liquefaction and no liquefaction.

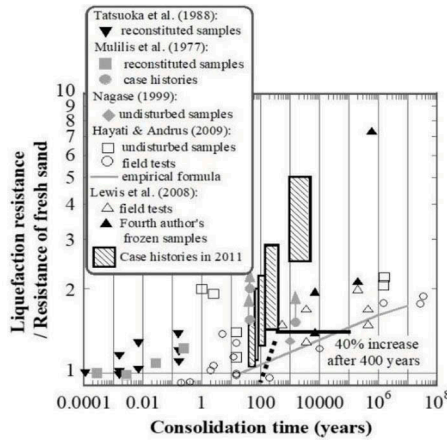


Figure 28. Increase of liquefaction resistance of soil with age under Japanese geological environment.

to be the upper bound of the border value; F_{Lmax} . This value is the upper bound because, otherwise, F_L value would be less than the border value throughout the profile and liquefaction should have occurred extensively, which is obviously contradictory against what happened in reality.

The obtained F_{Lmin} and F_{Lmax} were plotted against the soil age (Figure 27). Note that several more corrections were made in the F_L calculation. For details, refer to Towhata et al. (2016a). In Figure 27, the upper bound at sites without liquefaction is plotted by open symbols and the border between liquefaction and no liquefaction is below them as illustrated by downward arrows. In contrast, the lower bound at liquefied sites is plotted by solid symbols and the border is above them, as illustrated by upward arrows. The most likely border is between upward and downward arrows and is judged to be somewhere in the shadowed range. It is important that this shadowed range goes down with increasing soil age, suggesting that less liquefaction happens in aged soil in spite of the factor of safety less than 1.0. This means that actual liquefaction resistance is greater in aged soil than what is employed in the current design codes.

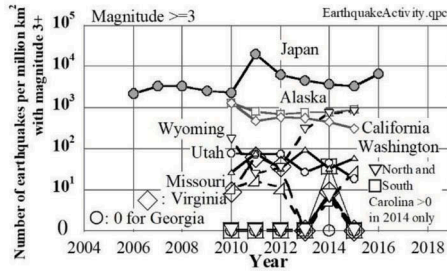


Figure 29. Difference in earthquake activities in Japan and USA (comparison of number of earthquakes per million km²) (Towhata, 2018).

Because the history of Tokyo started at the end of the 16th Century, older data was not available. This shortcoming was supplemented by studying Tsukiji area in Amagasaki City near Osaka and Kyo-ga-shima of Kobe. The former site was constructed at the beginning of the 17th Century and liquefied totally during the 1995 Kobe earthquake. The latter island was constructed at the end of the 12th Century and did not liquefy during the 1995 Kobe earthquake. For both, borehole data and earthquake motion records at nearby sites were available. Accordingly, the ageing effect in liquefaction phenomenon of sand was quantitatively captured for the time period of about 1000 years.

Figure 28 demonstrates the increase of liquefaction resistance with age, making the resistance of very recent soil being equal to unity. The results of the present study is shown by shaded rectangles whose size corresponds to the uncertainty in Figure 27. Basically the trend is consistent with results of other studies but may suggest more profound ageing in Japan than in North America. Towhata et al. (2016a) experimentally studied the mechanism of ageing and concluded that slow progress of grain movement (dislocation, change of fabric structure, change of force transmission among grains) is the cause of ageing. It is suggested that grain dislocation is promoted by minor earthquake shaking which has been called preshaking effects in other studies (Wichtmann et al., 2005). If this hypothesis is right, higher earthquake activities in Japan accounts for more progress of ageing than in North America (Figure 29).

4.2 Assessment of liquefaction vulnerability in residential land

The 2011 Tohoku earthquake triggered liquefaction in many residential lands. After the disaster, it became necessary to provide appropriate methodology to assess liquefaction vulnerability in residential land so that people and local community officers might be able to briefly assess the risk and undertake mitigation measures, if necessary. The author believed that conservatism should be eliminated from the methodology because people cannot afford cost for additional safety. To avoid forcing additional safety cost to people, the factor of safety, F_L , was calculated by using nearby ground motion records and considering the ageing effect (40% increase in resistance after 400-year age) based on many bore hole data that was obtained from both sites of liquefaction and no liquefaction.

An important issue was that minor liquefaction damage should be tolerated because light tilting, subsidence and others can be repaired at cost lower than soil improvement to the depth. Hence, three extents of house damage were defined and are illustrated in Figure 30 in which “A” means no damage, “B” are minor and “C” should have been avoided by soil improvement. At each site, thereafter, the factor of safety against liquefaction, F_L , was calculated along the bore hole log for further examination (Towhata et al., 2016b). The point of discussion was that the house damage is a consequence of the overall soil behavior and the F_L value at a single depth does not account for it. Hence, two indices (P_L and D_{cy}) for the overall behavior were calculated;

$$P_L = \int_0^{20} F(F_L)(10 - 0.5z)dz \quad (2)$$



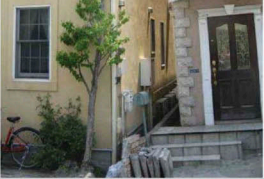
Damage extents	Photo of damage	Damage description
A: Nil - Minor		<ul style="list-style-type: none"> Minor or no distortion in road and houses.
B: Intermediate		<ul style="list-style-type: none"> Some sand ejecta, 10-30cm differential settlement in road surface, Tilting and subsidence of houses.
C: Major		<ul style="list-style-type: none"> Significant sand ejecta, Road distortion with >30cm differential settlement, Significant tilting and subsidence of houses.

Figure 30. Three extents of liquefaction-induced damage to house foundation (Towhata et al., 2016b).

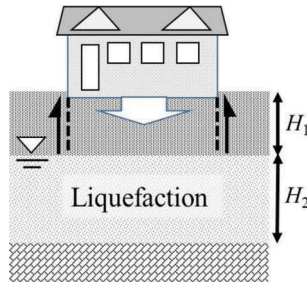


Figure 31. Significance of surface unliquefied crust resisting against punching failure of house foundation.

in which z is the depth in meter (Highway Bridge Design Code by Japan Road Association, Tatsuoka et al., 1980) and

$$F(F_L) = \begin{cases} 1 - F_L & (F_L \leq 1) \\ 0 & (F_L > 1) \end{cases} \quad (3)$$

while D_{cy} is vertical integration of cyclic shear strain amplitude, which is assessed by data of standard penetration tests and seismic load and is considered to be equivalent with the displacement amplitude at the ground surface (Recommendations for Design of Building Foundations by AIJ; Tokimatsu and Yoshimi, 1983; Tokimatsu, 1997). In addition, the thickness of the surface unliquefiable layer, H_1 , was taken into account. This parameter stands for the bearing capacity of surface soil that resists against the punching failure caused by the weight of houses (Figure 31).

Initially, it was difficult to obtain good correlation between the damage classification in Figure 30 and the combination of assessed indices (H_1 , P_L) or (H_1 , D_{cy}). This problem was overcome by examining the precise location of boreholes and the sites of reported damage which might be sometimes far from each other. In other extreme case, the reported depth of

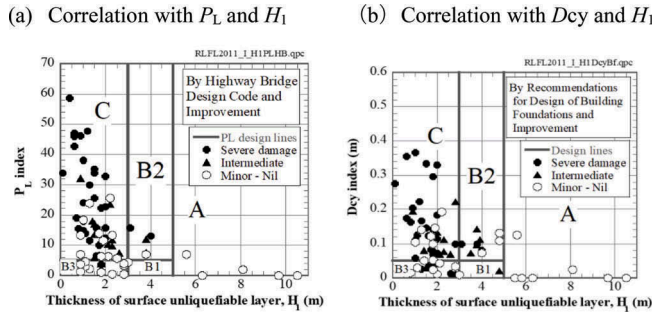


Figure 32. Correlation between damage extent of houses due to liquefaction and subsoil indices; B1-B3 are named after location in the graph. There is no difference in damage extent from what was shown in Figure 30.



Figure 33. Sand ejecta from the middle height of a levee (Yoshida River, Miyagi Prefecture).

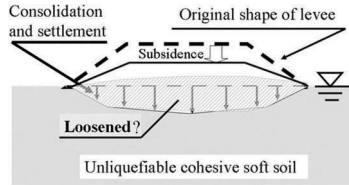


Figure 34. Mechanism of liquefaction inside a levee.

ground water table was 6 meter ($H_1 = 6\text{m}$) in a man-made island where the ground elevation is only 4 meters above sea level. This unrealistic depth of ground water was reported during borehole investigation probably when ground excavation was going on near the site and the ground water was pumped up for temporary purposes.

After detecting and thus removing irrelevant data from the study, a reasonable correlation was obtained between damage extents and the assessed liquefaction indices; no solid symbol in “A” category (Figure 32). These diagrams are used for brief evaluation of the quality of residential land subject to liquefaction risk (Towhata et al., 2016b). The difference between the present study and the well-known H_1 - H_2 diagram by Ishihara (1985) is the replacement of H_2 by P_L or D_{cy} . The author felt that H_2 parameter is determined simply by whether F_L is greater than or less than unity near the ground water level and might be too sensitive to minor difference in the original SPT data. Also, the mechanical role of H_2 layer is unclear. In contrast, P_L and D_{cy} are not so sensitive and expected to give stable conclusion. Although H_1 is sensitive as well, its mechanical role is clear as played in the resistance against punching failure. Hence, H_1 remains here.

5 VULNERABILITY OF RIVER LEVEES TO LIQUEFACTION

Sasaki et al. (2012) summarized the seismic damage of river levees in 2011 and indicated that most damage was related with liquefaction. Although traditional soil mechanics states that embankment has to be compacted for stability, the levees that are situated upon very soft soil cannot be compacted during construction because the sensitive subsoil may be disturbed and fail due to the impact. Consequently, the levee soil remains loose. This situation is aggravated by infiltration of rain water into the levee body. Consequently, a body of loose water-saturated sand (silty sand) is formed inside the levee. During the 2011 event, liquefaction occurred



Figure 35. Cross section of Tone River levee at Iijima Site.



Figure 36. 1-G shaking model of liquefaction-prone ground with vertical columns for restriction of cyclic shear strain.

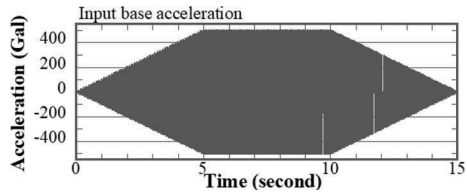


Figure 37. Time history of horizontal shaking in tests on mitigation effects of vertical group columns (10 Hz for 15 seconds).

inside the body of levees despite that the local natural subsoil was clay and unlikely to liquefy (Figure 23). Figure 33 shows sand ejecta from the middle height of a levee. This is an evidence that liquefaction is possible to occur at elevations higher than local ground water level. Figure 34 schematically illustrates the mechanism of liquefaction inside a levee. The water is supplied into loose sand in the levee either by infiltration of rain water or from the surrounding subsoil into the subsided part of the levee. Note that levee is often constructed upon soft clayey soil along a river channel; the clay is unlikely to liquefy but its consolidation settlement leads to submergence of loose levee bottom that comes down below the water table.

The 2011 Tohoku earthquake caused liquefaction in the levee body at many places. Although detailed risk assessment was insisted on after the disaster, the lack of information made it difficult. First, local geomorphological information does not help liquefaction risk assessment because the problem lies in the levee. Second, the soil condition inside the levee is hardly known due to the long history of levee construction. Along major rivers, the earliest and lowest levee was constructed before the 19th Century and the height has been increased several times without construction records available. Figure 35 illustrates a cross section of Tone River levee that was excavated for a research purpose. Note that the levee consists of many layers of past construction. More detailed investigation has to be conducted inside levee at a reasonable cost. Geophysical attempts of combined use of S wave velocity and electric conductivity to detect liquefaction-prone sand in a levee could not achieve desired resolution. In this regard, cone penetration and other probing are promising and desired.

6 INNOVATIONS IN MITIGATION OF LIQUEFACTION DISASTER

6.1 Use of group vertical columns on mitigation of liquefaction effects

In view of the significant liquefaction effects on our community, a numerous number of mitigation technologies have been investigated in the recent years. This chapter addresses some of them. They are characterized by reduced cost while allowing for a limited extent of ground deformation.

Two kinds of soil deformation associate liquefaction of subsoil. The one is the cyclic shear deformation during shaking which leads to high excess pore water pressure if its magnitude is profound. The other is the permanent deformation or flow failure that remains after shaking and is perceived as “damage” if significant. In the present study, it was aimed by a group of piles/columns in liquefaction-prone subsoil to reduce the cyclic deformation to avoid liquefaction and, even if liquefaction happens, to mitigate lateral flow.

Figure 36 shows a 1-G shaking model test in which model sandy ground with columns was shaken in a laminar box (Bahmanpour et al., 2019). The idea herein was that columns reduce cyclic strain during strong shaking, expecting that columns, which are constructed at cost lower than underground grid walls (Figure 58) and full grouting, reduce the damage at an appropriate cost. After the stage of Figure 36, sand was poured into the container and the entire model was submerged in water. Then the heads of the columns were connected by a template to prevent turn-over of columns during softening of subsoil. Figure 37 presents a typical time history of base acceleration.

Figure 38 shows the variation with time of excess pore water pressure that was measured among columns near the bottom of the model ground (60 cm below surface). The improvement ratio of AR=35% is defined by the cross section of columns divided by the horizontal area of ground. Although the pore pressure development ratio (max. pressure divided by the initial effective overburden pressure) is similar whether with or without columns, the rate of pore pressure rise (before 10 seconds of time) was reduced by columns and the extent of pressure dissipation after the peak value was accelerated. These two features make shorter the duration of adverse time period in which pore water pressure is very high. In Figure 39, shaking was repeated on the same model ground by increasing the amplitude of acceleration while maintaining the shape of the time history (Figure 37). It is shown that pore pressure was reduced by increasing the area ratio (closer spacing among columns).

Further study was made of the effects of columns on reduction of lateral soil flow as a consequence of liquefaction (Towhata et al., 2015a; Takahashi et al., 2016). The major point of concern was the benefit of irregular configuration of columns that maintains the same number of columns and the same cost of construction but achieves better reduction of liquefaction effects. In Figure 40, the conventional square and triangular column configurations allow relatively free cyclic shaking of soil and easier flow of soil among columns in case of liquefaction. In contrast, the “irregular” configuration does not have such free direction of motion and is expected to reduce both cyclic strain amplitude and flow displacement. The irregular configuration is composed of square unit geometry and should not be confused with a “random” geometry that is difficult to install in field practice.

A series of centrifugal model tests (50G) have been conducted at the Port and Airport Research Institute in order to verify the mitigative effects of the irregular configuration. Figure 41 illustrates one of the tested models and Figure 42 shows an example of input shaking.

Figure 43 compares the distribution of lateral displacement. In this figure, Case 0 had no column and the maximum input acceleration was 150 cm/s². In contrast, Case 3 employed the

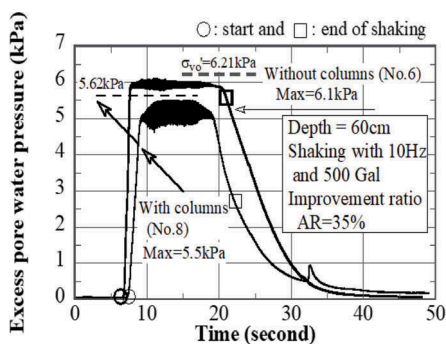


Figure 38. Time history of excess pore water pressure with and without columns.

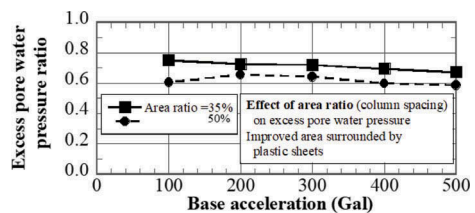


Figure 39. Effect of area ratio of columns on reduction of excess pore water pressure.

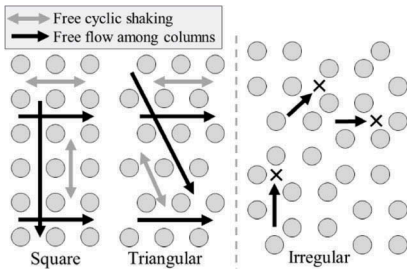


Figure 40. Plan view of three column geometries.

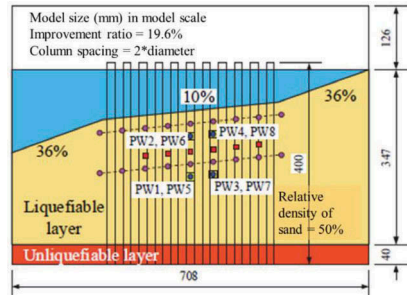


Figure 41. Centrifuge model test on irregular columns configuration embedded in a liquefiable slope.

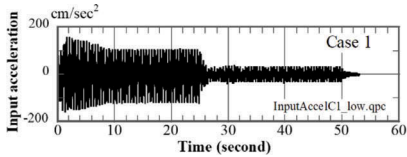


Figure 42. Example of input acceleration for tests on irregular column configuration.

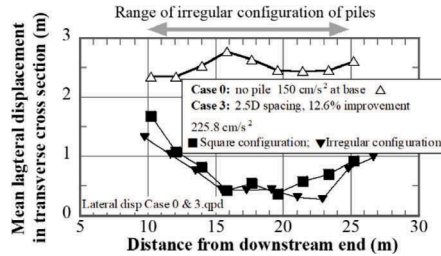


Figure 43. Effects of vertical columns on reduced lateral flow of liquefied slope.



Figure 44. Excavated shape of columns with head connection (full-scale model, after Dr. Naoki Takahashi).

column spacing = $2.5 \times$ column diameter (12.6% improvement) and the input shaking was as strong as 225.8 cm/s^2 . In spite of this strong shaking, the columns successfully reduced the lateral displacement. Note that the difference between tests with square and irregular configuration was not significant. Furthermore, the head of columns has to be connected together in order to prevent turnover of the entire column group (Figure 44).

6.2 Extensive installation of drainage pipes

Because of the significant liquefaction effects on houses (Figure 18), need was strongly felt for simple soil improvement under existing houses. Attention was paid, accordingly, to such technologies as injection of air bubbles into subsoil (Okamura et al., 2011) and sheet pile walls around individual house foundation (Yasuda, 2013a & b). In this regard, Razouli et al. (2016) studied the possibility of installed drain pipes that dissipate the excess pore water pressure quickly under existing houses.

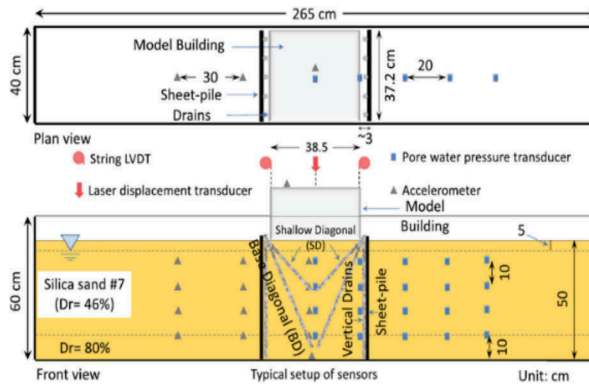


Figure 45. Schematic diagram of typical experiments and position of drains.

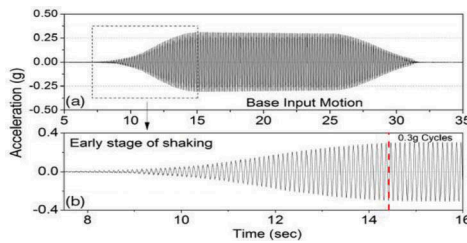


Figure 46. Base input motion (a) the whole shaking of 10 Hz and 300 cm/s^2 ; (b) the early stage of shaking for considering weaker earthquakes (equivalent 15 cycles).

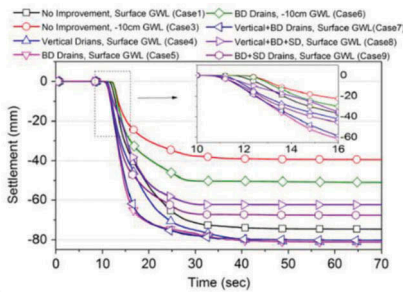


Figure 47. Recorded time histories of house settlement with different mitigation measure (no sheet pile wall).

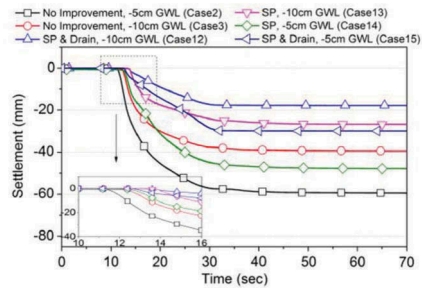


Figure 48. Recorded time histories of house settlement with different mitigation measures (with sheet pile wall).

Figure 45 demonstrates one of the tested models in which a house model was placed at the center and three kinds of mitigation were installed; diagonal drain pipes at shallow (SD) or deep (BD) elevations, sheet pile walls around the house foundation with vertical drains and lowering of ground water level. Because of the existing house at the surface, drains have to be installed in the diagonal directions. In the series of tests, three technologies were investigated separately or in combination. Figure 46 plots the input acceleration time history. Because the study was made after the gigantic earthquake of magnitude = 9, the number of shaking cycles is many. To take account of earthquakes of smaller magnitude as well, test data will be interpreted at 16 seconds after 15 cycles of 300 cm/s^2 as well as at the end of the whole shaking.

Figure 47 compares the time history of house settlement with different kinds of mitigation measure. The most effective mitigation was lowering of ground water by 10 cm which is about

25% of the house size. Noteworthy is that lowering of ground water level (GWL) for a single house requires underground walls around the house which increases the cost in practice. If lowering is executed for an entire community, care must be taken of possible consolidation settlement in cohesive subsoil. For this reason, the conclusion from this figure is that the combination of drains (SD, BD and vertical) without GWL lowering is the most effective. Only vertical and BD drains without GWL lowering was not effective at all. Further comparison was made in Figure 48 in which cases with sheet piles (SP) around the house foundation are plotted. In this figure, SP with vertical drains attained the best performance; see Case 15 in which settlement is small in spite of shallow GWL (-5cm).

7 PROTECTON OF EXISTING RESIDENTIAL AREAS FROM FUTURE EARTHQUAKE DISASTER

7.1 Tsunami

One of the lessons learnt from the 2011 tsunami disaster was that sea wall is not a fully reliable safety measure. If tsunami is higher than wall, overtopping results in a catastrophic situation. Therefore, the new principles of safe community are “evacuation” and “high ground level” that are combined with reasonably high sea wall. The high ground elevation prevents catastrophic inundation in case of extremely high tsunami, while sea wall stops more frequent lower tsunamis.

Figures 49 and 50 illustrate the on-going reconstruction of Rikuzen-Takata town; see Figure 8 for the damage. In Figure 49, a new town center together with the new town hall have been relocated to the top of a hill. Following this stage, re-construction of the former town area, which was inundated by tsunami water, resumed by elevating the ground level to 9-12m above sea level. Relocation and elevating are executed over an area of 186.1 ha. Its budget is 53.69 Billion Yen for population of 1450 families and 4300 people (Rikuzen-Takata City, 2016). Thus, the cost is approximately 34.4 million Yen/family or 12.5 million Yen/person (1 Euro = 134 Yen on Dec. 10, 2018). Moreover, the railways in this region that were washed away by tsunami are reconstructed as a “bus rapid transit” (Figure 51) in which bus can run on the designated road and the maintenance cost is lower than that of railway.

7.2 Liquefaction in residential district

Tens of thousands of existing houses were affected by subsoil liquefaction in 2011 because they were situated on young loose cohesionless deposits. Since the effect was as vast as that of tsunami damage (Section 7.1), similar public supports for reconstruction of the liquefaction-prone community was considered necessary. However, the public principle is that the damage restoration of private properties is the responsibility of individual people and that the public money should not be spent on it. Moreover, the previous regulation assumed the responsibility of seismic safety of residential land to the owners who purchased the land; not to the developers or the contractors.

After a long negotiation with the financial ministry, this difficulty was overcome by pointing out that liquefaction in private lands affects the public properties such as roads and lifelines (Figure 52). Because liquefaction in subsoil occurred uniformly irrespective of the



Figure 49. New town center at top of hill (Rikuzen-Takata, March 2017).



Figure 50. Raising ground level by 15 m in former town area (Rikuzen-Takata).



Figure 51. Reconstruction of local public transport by bus rapid transit (Kesen-numa).

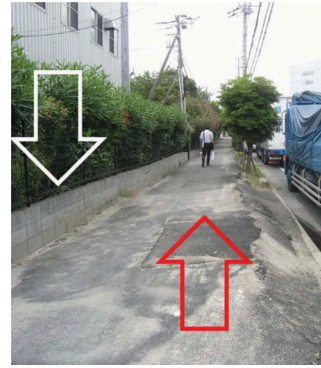


Figure 52. Heaving of road induced by subsidence in private land (Urayasu, Chiba Prefecture).

border between private and public properties, it was decided that liquefaction mitigation works in private land should be installed by 50% public and 50% private expenses. Because people are not familiar with technical issues, the ground improvement projects have been conducted under the initiative of local governments. Another point is that the ground improvement has to be conducted on a community basis in which tens or hundreds of families in town blocks unanimously agree to join the project. This requirement was found very difficult to fulfill later. Note that relocation of liquefaction-prone community to safer places, which was the case in Christchurch of New Zealand, was not practiced in Japan because people preferred to stay in the same place and local governments did not want to lose tax payers.

Several municipalities started to prepare for this public-private framework. However, some people did not want to spend money on ground improvement because they could not afford it, they were afraid of future maintenance cost (operation of ground water pumping in case of lowering water level) or they had already installed expensive mitigation measure under their own houses.

The choice of liquefaction mitigation technology was entrusted by people to local governments. Under this situation, only those technologies that had been verified or had been used in practice were eligible. In other words, technologies under development or research such as those referred to in Chapter 6 had to be ruled out. Accordingly, only two remained which were ground water lowering and installation of underground grid walls.

Ground water lowering was previously employed in Tsukiji District of Amagasaki City which is the western neighbor of Osaka. The 1995 Kobe earthquake caused liquefaction here and most houses were demolished. Earth was then filled by 1.5 m on the surface and pipes were installed to drain ground water (Suwa and Fukuda, 2014). Earth filling was a compensation for the long-term consolidation settlement that used to be serious due to industrial water pumping until 1960s and had made the ground surface even lower than the sea level. Since industrial pumping was banned in 1960s, the ground water level had been rising, making the local soft clay over-consolidated. Because of this, earth filling and limited lowering of ground water level did not cause consolidation settlement (Figure 53). The liquefaction mitigation project in Tsukiji was completed in 2004 which is 9 years after the Kobe earthquake (Amagasaki City Government, 2007). After 2011, several municipalities successfully achieved unanimous agreement of people on ground water lowering and the measures were installed (Figures 54 and 55); refer to Itako City Government (2013) and Kokusho (2014) as well as Yasuda and Hashimoto (2016).

7.3 Liquefaction in Urayasu City, Chiba Prefecture

9154 houses were affected by liquefaction in Urayasu City. Most parts of this city (Figures 14 and 24) were constructed in 1960s and 70s by dredging of marine bed and reclamation of the dredged silty sand in shallow sea water. The liquefaction resistance of this sand was obtained



Figure 53. No settlement problem in Tsukiji of Amagasaki after ground water lowering.



Figure 54. Hinode District of Itako City where ground water is drained by gravity flow through installed pipes.



Figure 55. Discharge of ground water into river in Kuki City (photo provided by Prof. J. Koseki).

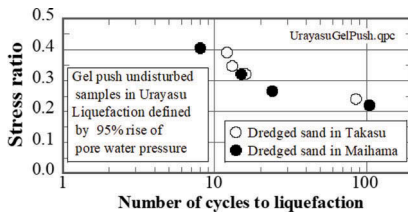


Figure 56. Liquefaction resistance of undisturbed samples collected at two places in Urayasu by gel push sampling developed by Mr. K. Sakai of Kisojiban Consultants, Tokyo.

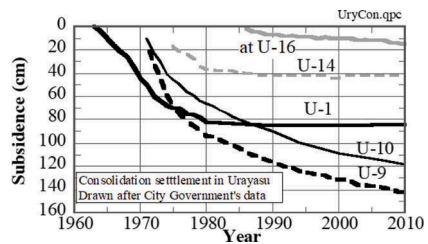


Figure 57. Consolidation settlement in recent land reclamation of Urayasu.

by using undisturbed samples collected by gel push sampling (Figure 56). Because the area is on the mouth of big Tone River, whose channel was here until new channel was constructed in late 17th Century, the man-made island in the city has been underlain by 40-meter deposit of soft alluvial clay. Hence, the man-made island in the city has been annoyed by consolidation settlement for decades (Figure 57). The memory of settlement is still vivid among people and repetition of settlement due to ground water lowering was not appreciated. Under the democratic framework, therefore, the city government could not pursue ground water lowering.

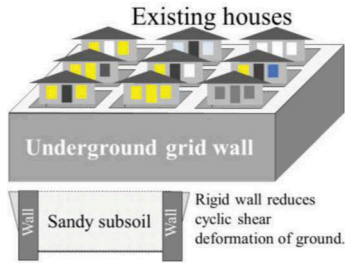


Figure 58. Conceptual illustration of the role played by underground grid wall.



Figure 59. Narrow space between two adjacent houses.

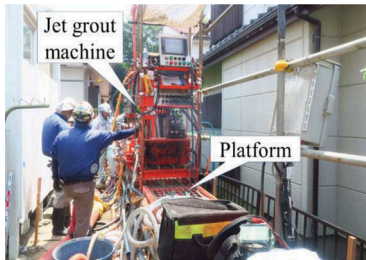


Figure 60. Jet grouting by a small machine placed on an elevated platform (August, 2018).



Figure 61. Construction of underground wall under street by mechanical mixing.

The alternative technology was installation of grid-type underground walls that were constructed by mixing cement and local soil by mechanical mixing or jet grouting. Certainly, this option was more expensive than ground water lowering. Figure 58 schematically shows the grid wall that are installed in a narrow space among houses. The rigidity of the grid wall reduces the cyclic shear deformation of subsoil during earthquakes and mitigates the risk of liquefaction. This technology became popular after its success in Kobe Harbor in 1995. Nevertheless, Urayasu was its first application to subsoil under “existing” houses that are fragile and do not allow very small distortion or tilting that affect health of residents. Very narrow space for underground wall construction was another big issue (Figure 59). After discussion, it was decided to select the grid wall as the measure and design started. The goal of design was “little damage in houses under the same strong earthquake as the one in 2011”. It was not the goal to insure zero damage in any future earthquakes.

Accordingly, the cost evaluation on ground improvement in the private land was such as 6 million Yen per house. As stated before, its 50% was paid by the national government and the local government offered supports of about 17% so that the people’s payment might be not more than 33%. Based on this condition, many meetings were held between the administration and the residents, aiming at unanimous agreement of people in 16 districts (4103 houses) in the city. Finally, three districts with 471 houses (only!) reached unanimous agreement and preliminary works started on sites. Figure 61 illustrates a local street under which wall was successfully constructed by powerful mechanical cement mixing.

The works, however, had to be stopped in April, 2017. The first reason was non-uniform soil condition in the city. Jet grouting did not work well in clay parts. The second reason was detecting many embedded plastic drains that were not expected to be there during design. They had been installed at an interval of several meters for promotion of consolidation settlement probably in 1970s when the land reclamation took place. Rotating jet grout machines caught drains (Figure 62) and grout could not be injected into subsoil. Consequently, stable and continuous grid wall was not able to be constructed.



Figure 62. Plastic drain caught by rotation of jet grouting machine.



Figure 63. Successful grouting shown by solidified soil cores.

Nowadays, construction engineering is not respected by people. Its public image is far from that of the advanced science and technology. Moreover, media frequently reports construction related with political corruption. The author has been advocating that more efforts are required to improve the public image. In this regard, what the Urayasu project had to do was to overcome the technical difficulty irrespective of the possible increase of cost and keep the promise with people. Therefore, the author, who was the Chair of the technical advisory committee of the project, visited the sites more than 30 times in summer of 2017, free of charge, and encouraged engineers to overcome the problem. Consequently, it was decided to increase the grouting pressure, run the jet grouting procedure twice at sites and inspect possible drain effects so that drains might be removed from the machine and grouting might be run one more time. After this decision, jet mixing worked well and Figure 63 shows a core sample of solidified clay that was continuous throughout the clayey subsoil. The negative effect of the solution was elongated construction time and cost. The national government decided to provide additional financial supports and people were not required to spend more expense than the original plan.

Considering the elongated project period, people's unanimous agreement was required again in early 2018 and the rate of agreement dropped to 78%. Although this still meant that absolute majority supported the project in the three districts, the project had to be cancelled in two districts with 393 and 45 houses, respectively. Only one district with 33 houses accepted the project and ground improvement was carried out in 2018 (Figure 60). The total construction cost in this district is 1.147 Billion Yen for both streets and private lands. The difficulty in other districts was that people did not want to live in "construction site" any more. Further, seven years had passed since the earthquake and people's concern had decreased.

8 PROTECTION OF BURIED LIFELINE FROM LIQUEFACTION DAMAGE

The 2011 earthquake and induced liquefaction destroyed embedded life lines at many places. In the modern times, lifeline is an essential component of urban community and its seismic vulnerability is a big threat to the resilience of cities in seismically active regions. The author paid special attention to liquefaction resistance of sewage pipelines because possible change of the pipe gradient due to backfill liquefaction significantly affects the flow of waste water under gravity.

The damage of sewage lifelines is classified into that of manhole (Figure 16) and floating of pipes (Figure 17). Because the mitigation technology for manhole has been investigated by Orense et al., (2003), Kiku et al. (2006), Tobita et al. (2011) and Yoshida et al. (2008) among others, the author put emphasis on existing embedded pipelines (Otsubo et al., 2016a and b). It was attempted therein to avoid overall excavation and improvement of liquefaction-prone backfill soil around the pipe and thereby to reduce the cost.

mitigation.

Figure 64 illustrates one of the innovations by which floating of pipe is prevented by inserting a "horn" between the pipe and the surface pavement. Herein, the backfill soil is supposed

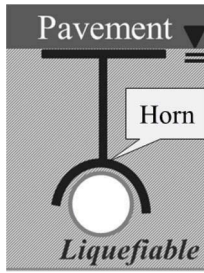


Figure 64. “Horn mechanism” to prevent floating of pipe.

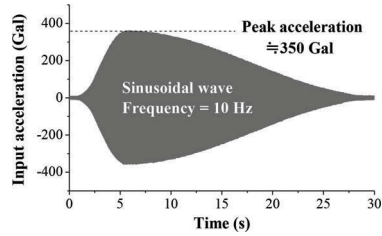


Figure 65. Input acceleration record in 1-G model tests on pipeline.

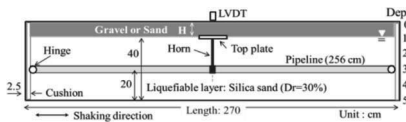


Figure 66. 1-G shaking model for pipeline tests (pipe diameter=6cm).

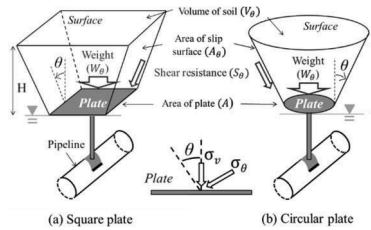


Figure 67. Details of prevention mechanism by overlying unliquefied layer.

to liquefy but pipe stays at the original position because floating is prevented by the horn. Note that this idea requires excavation only at the places of horn installation, which is less expensive than other measures such as overall excavation and cement mixing of backfill soil, or placement of better backfill materials.

1-G shaking tests were conducted on prevention of floating of a pipe embedded in liquefiable backfill sand. Figure 65 shows the input motion which has the amplitude of 3.5 m/s^2 and 10 Hz frequency. The strong acceleration was chosen by considering the social demand after the big earthquake. The high frequency was employed from the similitude viewpoint. The relative density of sand was 30%, which produces similar dilatancy as the prototype in spite of reduced stress level. The overall configuration of a tested model is illustrated in Figure 66. The pipe model was embedded in liquefiable sand and its two ends were connected to the soil container by hinge (manhole connection in reality). In the middle, the pipe floating was prevented by a column (horn in practice) and a top plate (square or circular in shape; see Figure 67) which is overlain by an unliquefiable layer of gravel or sand (road pavement in practice) or a stationary beam (Case *H1* with zero displacement as the control case). Friction angle of the medium dense gravel, loosely packed gravel and sand are chosen to be 40° , 35° and 30° , respectively. As illustrated in Figure 67, the prevention of floating is developed by the weight of unliquefied soil and the shear resistance along the (punching) failure plane. Herein, values of A and H were varied and many tests were run. The oblique angle of the failure plane (θ) will be determined by referring to the test results.

Figure 68 shows an example record of the force that developed in the horn structure supported by a rigid beam for zero floating. By eliminating the high-frequency component, the maximum uplift force was determined at 74.3 N. Another case was run without horn and the ultimate floating was 3.1 cm. In case of sandy or gravelly surface layer with horn, the floating was smaller and the horn was compressed by less extent of force ($<74.3\text{N}$). The maximum possible force of 74.3 N was compared against the uplift resistance (combination of weight and shear resistance in the surface layer) in order to assess the factor of safety against floating.

Figure 69 illustrates the relationship between the factor of safety and the reduction of floating displacement in which 100% stands for null floatation. The greater factor of safety results

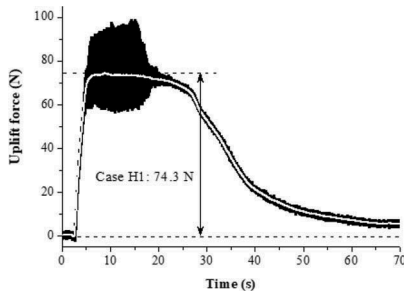


Figure 68. Example time history of uplift resistance measured in hone structure.

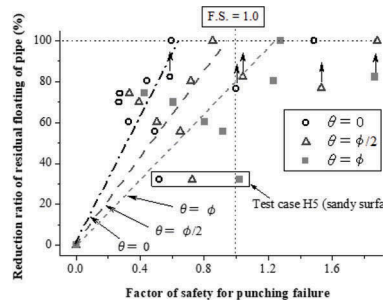


Figure 69. Relationship between the factor of safety and the reduction of floating.



Figure 70. Flow-in of liquefied backfill sand into separated sewage pipes (photograph by Urayasu City).

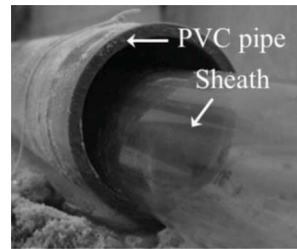


Figure 71. Sheath pipe inside a PVC pipe model.

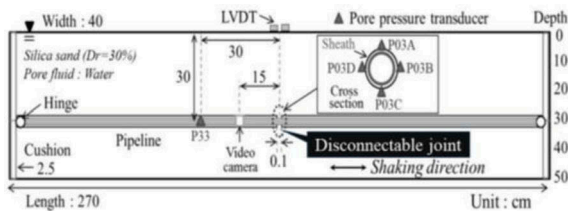


Figure 72. Configuration of model ground for test with inserted sheath pipe.

(a) Without sheath (b) With sheath

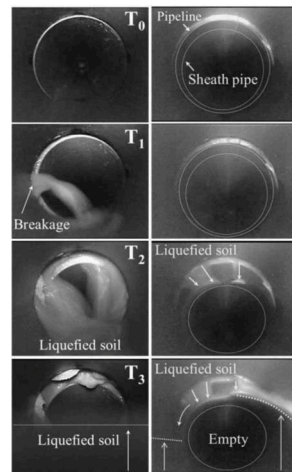


Figure 73. Situation inside an embedded pipe during shaking.

in more reduction of floatation. In this figure, the factor of safety obtained by $\theta=\varphi$ gives 100% reduction at the factor of safety = 1.0. Thus, the design of punching resistance is assessed by $\theta=\varphi$ in the surface layer of road pavement.

One of the frequent damage mechanism of sewage pipeline during earthquakes is the flow-in of liquefied backfill into pipe through disconnection at pipe joints (Figure 70). To avoid

this, slip lining of a sheath pipe inside an existing pipe (Figure 71) seems promising (Matthews et al., 2013) because sheath pipe prevents flow-in of external sand and provides sufficient space to flow of water. Sheath is a useful measure also for rehabilitation of aged buried pipes.

Shaking tests were run on the model in Figure 72 where two segments of pipes were loosely connected so that breakage might be induced there and liquefied sand might flow in. Figure 73 illustrates the situation inside the pipe that was captured by a video camera during shaking. Obviously, liquefied sand could not come into the sheath pipe.

9 PROFESSIONAL ENGINEER FOR GEOTECHNICAL EVALUATION

The 2011 earthquake exhibited that many residential lands are prone to seismic risk (Figures 18, 19 and 30). Residential land is vulnerable to further risk due to heavy rain, debris flow and landslide as well (Figure 74). People are living there without recognizing the situation. They purchase land considering only the price, comfort to live and convenience in life. After disasters, they lament that there was no way to be informed of the risk, although many municipalities provide hazard maps to residents. In this situation, the Japanese Geotechnical Society established the Japanese Association for Geotechnical Evaluation together with several other institutions in order to promote the new qualification of geotechnical evaluator (Towhata and Nakamura, 2015b).

The title of “Professional Engineer for Geotechnical Evaluation (PEGE)” is awarded to those who wish to work for the safety of people and have sound knowledge of geotechnical engineering as well as practice of residential land construction. Knowledge on local geomorphological history is important as well. Their basic qualification is verified by professional titles that they have obtained such as “Professional Engineer”, “Registered Architect” and “Civil Engineering Works Execution Managing Engineer” among several others. The PEGE title is awarded to those who have passed additional examination on practice of residential land construction and is valid for five years, followed by further extension. In early 2018, this title was officially certified by the national government. Note that PEGE is not a voluntary title. PEGEs are expected to work as professional engineers who earn reasonable income from clients.

10 ROLES OF GEOTECHNICAL ENGINEERING TOWARDS SOLVING THE PROBLEM OF FUKUSHIMA NO.1 NUCLEAR POWER PLANT

One of the severest disasters caused by the 2011 Tohoku earthquake was the tsunami disaster in the Fukushima No.1 Nuclear Power Plant. Note that the present paper calls this plant



Figure 74. Consequence of rain-induced debris flow in Hiroshima, 2014.



Figure 75. Piles of plastic bags to store radioactively contaminated surface soil around the power plant (January 15th, 2019).



Figure 76. Super heavy mud water for radioactive shielding (study at Waseda University).

“Fukushima No.1” in place of the official name of “Fukushima Daiichi” because “Daiichi” means “No.1” and better understanding is achieved by the latter. While there is a wide range of arguments about the future of nuclear power technology, the author understands that the solution of the Fukushima No.1 problem is of unanimous support from people. It is a national goal to solve this nuclear disaster and return the area safely to local people.

As is well known, the nuclear disaster was caused by the unexpected height of tsunami. Shaking toppled electric transmission towers and the external power supply stopped. However, internal power (battery and diesel generator) was supposed to survive the earthquake because they were placed in the basement where shaking effect was least. Unfortunately, the tsunami was higher than the design height and the internal power supply was destroyed by inundation in the basement. Cooling of reactors stopped, the nuclear fuel melted down, the containers of reactor were damaged, the hydrogen gas leaked out of the containers and got exploded. Furthermore, air, ground water and sea water were contaminated radioactively, local people had to evacuate and, consequently, the community was lost. Fortunately, other nuclear power plants in the same coastal area were able to survive. Within a few years after the disaster, it became evident that the problems to be solved are so complicated that many different fields of science and technology have to collaborate on this for the next 40 years or more.

Geotechnical engineering is expected to play such important roles as cleaning of contaminated soils around the power plant (Figure 75), control of radioactivity in and around the foundation of power plants and final treatment of debris (molten fuel and other radioactive wastes in the destroyed reactors) and radioactive wastes. Moreover, removal of debris from the reactors is similar to excavation or rock coring in geotechnology. The whole efforts to solve the problem is called decommission. Accordingly, the Japanese Geotechnical Society resumed efforts to provide core engineers to the decommission of Fukushima No.1 Plant for the next 40 years (Komine, 2017).

One of the technical innovation of the said activity is super heavy mud water (Figure 76). Similar to well-known bentonite water, this liquid is produced by mixing special clay with water. Because of its high mass density (exceeding 2.5 Mg/m^3), it can shield (reduce the intensity of) γ ray, while its high water content (50-90% of volume occupied by water) helps shield neutron beam. Moreover, its fluid nature and low permeability make it possible for the mud water to flow into small parts of the damaged reactors and stop leakage of radioactive water (Komine et al., 2016; Yoshikawa et al. 2017). It is noteworthy that this material can be produced and supplied in a massive scale to meet the needs of real construction project. Thus, the super heavy mud water will contribute to maintain the radioactive safety in the decommission site for 40 years.

Development of human resource who will be engaged in decommission during the next 40 years is an essential part of the activity. It is aimed therein to produce civil/geotechnical engineers who have reasonable knowledge of nuclear engineering. They need to know well about radioactivity and structure of nuclear power plants. In 2018, the first version of teaching material was completed for one-semester subject “geotechnical engineering for decommission”

that is to be used in university education. It puts emphasis on construction practice and consists of the following topics:

basics of radioactivity, overall scope of geotechnical engineering for decommission, geomaterials, geoenvironmental engineering, waste treatment, super heavy mud water, ground water control, final treatment of nuclear wastes, effects of nuclear accident on human health and brain storming.

All the contents emphasize contribution to decommission. Moreover, a technology map was made in which information on technologies that facilitate decommission project was collected and engineers can search details according to their needs (Towhata et al., 2018).

11 TREATMENT OF DISASTER WASTE

The earthquake left behind a huge amount of waste that were destroyed buildings, households, radioactively-contaminated soil etc. (Inui et al., 2012). Prior to treatment, they had to be classified in accordance with their size and properties. Although detailed discussion is desired on this issue, there is no more space in this paper.

12 EMERGING PROBLEMS

Civilization changes with time. Life style of people are not same as before. The recent trend is increased desire of people for safety. Because of this, new earthquake problems become important one after another.

The 2016 Kumamoto earthquake sequence, Japan, of Mw=6.2 and then 7.0 demonstrated the difficulty in coping with two consecutive strong earthquake shakings; the first one caused partial damage in structures and slopes, while the second one 28 hours later triggered their total collapse. Should we prevent any partial damage during such a rare first event for the safety during the second event? It is too costly. The same earthquakes produced fault rupture in a populated area of Mashiki Town.

The 2018 Hokkaido Eastern Iwuri earthquake of Mw=6.6 revealed the weakness of private residential fill in which collapse has been repeated during many past earthquakes. Failure of slopes that comprised of volcanic ash is another problem. Sapporo City experienced liquefaction problem in its residential area during this earthquake (Figure 77). After learning negative lessons from Urayasu and other areas, the Sapporo City Government put emphasis on quick execution of ground improvement project under existing houses. Accordingly, the design was completed within 6 months after the earthquake and project will start in April, 2019, after snow melt. The subsoil under houses will be improved by injecting colloidal silica.

Further, the 2018 Sulawesi earthquake of Mw=7.5 in Indonesia was associated with submarine landslides that induced tsunami. Also, gentle slopes flowed hundreds of meters at 4 places and claimed hundreds of casualties. People's desire for safety is far from satisfaction.

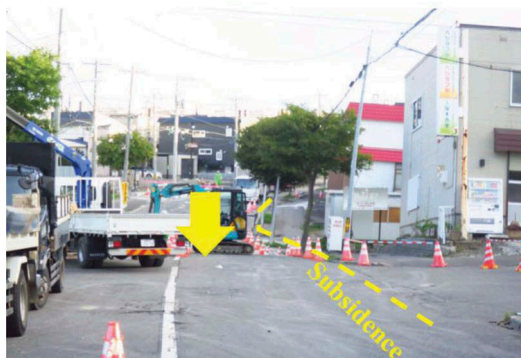


Figure 77. Liquefaction-induced ground distortion in residential area of Sapporo in 2018.

13 CONCLUSION

This paper summarizes a range of geotechnical efforts and contributions towards the recovery from the seismic disaster in 2011. In contrast to what was done in the 20th Century, the activities after 2011 are more related with people's property (liquefaction under houses), less expensive but long structures (river levee and lifeline) and completely new problems (nuclear accident). Efforts so far made are not complete and are required to be continued in the coming decades.

ACKNOWLEDGMENT

The contents of this paper are based on many efforts of colleague geotechnical engineers. First, the contributions of many former civil engineering students of University of Tokyo are appreciated. Collaboration with and supports provided by Ministry of Land, Infrastructure, Transport and Tourism was essential. Centrifugal model tests at the Port and Airport Research Institute provided many valuable findings. Earthquake acceleration records collected by K-NET is always useful. Development of geotechnical engineering for decommission is supported by a project named "Human Resource Development and Research Program for Decommissioning of Fukushima Daiichi Nuclear Power Station" under the auspices of Ministry of Education, Culture, Sports, Science and Technology. The author expresses his sincere appreciation to those efforts, supports and collaboration.

REFERENCES

- Amagasaki City Government. 2007. Project for restoration of Tsukiji Community after earthquake disaster (in Japanese).
- Bahmanpour, A., Towhata, I., Sakr, M., Mahmoud, M., Yamamoto, Y. & Yamada, S. 2019. The effect of underground columns on the mitigation of liquefaction in shaking table model experiments, *Soil Dynamics and Earthquake Engineering*, 116(1):15-30.
- Endo, K. & Mazereeuw, M. 2015. Historical study on geographical features of shrines in town of Minami Sanriku, Miyagi Prefecture, *Journal of the Japanese Institute of Landscape Architecture*, 78 (5):693-696 (in Japanese).
- Hatori, T. 1975 Tsunami magnitude and wave source regions of historical Sanriku tsunamis in Northeast Japan, *Bulletin of Earthquake Research Institute, University of Tokyo*, 50: 397-414 (in Japanese).
- Hayati, H. & Andrus, R.D. 2009. Updated liquefaction resistance correction factors for aged sands. *J. Geotech. Geoenviron. Eng., ASCE* 135(11): 1683-1692.
- HERP (Headquarters for Earthquake Research Promotion) 2009. Long-term evaluation of seismic activities in the region from Off-Sanriku to Off-Boso (revised), Report by Geological Investigation Committee (in Japanese).
- Housner, G.W. 1963. An engineering report on the Chilean earthquakes of May 1960, *Bulletin of the Seismological Society of America*, 53(2): 219-223.
- Inui, T., Yasutaka, T., Endo, K. & Katsumi, T. 2012. Geo-environmental issues induced by the 2011 off the Pacific Coast of Tohoku Earthquake and tsunami, *Soils and Foundations*, 52(5),856-871.
- Ishihara K. 1985. Stability of Natural Deposits During Earthquakes, Theme Lecture at 11th ICSMFE, San Francisco, Vol. 1:321-376.
- Ishihara, M. & Sasaki, T. 2012. Relationship between age of ground and liquefaction occurrence in the 2011 Great East Japan earthquake. *Proc. Int. Symp. Engineering Lessons Learned from the 2011 Great East Japan Earthquake*, Tokyo, 771-776.
- Itako City Government. 2013. Report on liquefaction mitigation project in Hinode District, <http://www.city.itako.lg.jp/page/page002163.html> retrieved on Dec. 11, 2018 (in Japanese).
- JMA (Japanese Meteorological Agency). 2011. On The 2011 off the Pacific coast of Tohoku Earthquake (Ver.15), Press release, Retrieved Nov. 28 2018 (in Japanese).
- Kawasumi, H. & Sato, Y. 1949. Characteristics of ground deformation, tsunami, seismic intensity and damage extent caused by the 1946 Nankai earthquake, Record of 1946 Nankai earthquake disaster, Ed. Kochi Prefectural Government, 18-52 (in Japanese).

- Keino, C., Kohiyama, M. & Sonobe, T. 2011. Health damage of residents caused by liquefaction damage of houses - Examples in Mihama of Chiba during the East Japan Earthquake Disaster, Annual Convention of JAEE, 80-81 (in Japanese).
- Kiku, H., Fukunaga, D., Matsumoto, M. & Takahashi, M. 2006. Shaking table tests on countermeasures against uplift of manhole due to liquefaction. Annual Conference of JGS, 2:1889-1890 (in Japanese).
- Kitahara, M. & Uno, R. 1965. Relationship between tilting of floor and dizziness - Case history study in tilting building in Niigata, *Practica Oto-Rhino-Laryngologica*, Society of Practical Otolaryngology, 58 (3):145-151 (in Japanese).
- Kohiyama, M. & Keino, C. 2012. Health disturbance of residents in houses tilted due to liquefaction during the Great East Japan earthquake. 15th World Conf. Earthq. Eng., Lisbon.
- Kohiyama, M., Keino, C. & Sonobe, T. 2012. Questionnaire Survey on Health Disturbance of Residents in Mihama Ward, Chiba City Who Suffered Housing Damage due to Liquefaction, *Journal of Institute of Social Safety Science*, 17: 1-7 (in Japanese).
- Kokusho, T. 2014. Liquefaction damage and restoration in Itako City, Report on the Great Est Japan Earthquake Disaster, Fundamental Aspect 3 “Geohazards”, 261-267 in DVD publication□(in Japanese)
- Komine, H. 2017. Creation of decommission technology and collaboration with nuclear engineering, *ATOMOS*, Atomic Energy Society of Japan, 59 (4):11-13 (in Japanese).
- Komine, H., Towhata, I. & Narushima, S. 2016. Environmental geotechnics and education initiatives for recovery from the Fukushima I Nuclear Power Plant Accident, *Japanese Geotechnical Society Special Publication*, 2:1982-1985.
- Kotoda, K. & Wakamatsu, K. 1988. Liquefaction and Resulting Damage to Structures during the Chiba-ken-Toho-Oki Earthquake, *Monthly Magazine*, Japanese Society of Soil Mechanics and Foundation Engineering, 36 (12):19-24 (in Japanese).
- Lewis, M., Arango, I. & McHood, M. 2008. Site characterization philosophy and liquefaction evaluation of aged sands — a Savannah River site and Bechtel perspective, *Proc. Conference “From Research to Practice in Geotechnical Engineering”*, *Geotechnical Special Publication*, New Orleans, USA, 180: 540-558.
- Matthews, J., Condit, W., Sinha, S., Maniar, S., Sterling, R. & Selvakumar, A. 2013. State of Technology for Rehabilitation of Water Distribution Systems, Report to EPA/600/R-13/036, p.31.
- Matsuura, S. 2013. Tsunami effect on shrines during the Tohoku earthquake in March 2011, *Hydrological Science*, 57 (3):168-186 (in Japanese).
- Mulilis J.P., Mori K., Seed H.B. & Chan C.K. 1977. Resistance to liquefaction due to sustained pressure. *Proc. ASCE*, 103(GT7): 793-797.
- Nagase, H., Shimizu, K., Hiro-oka, A., Mochinaga, S. & Ohta, M. 1999. Increase in liquefaction strength of sandy soils due to aging, *Proc. 34th Japan National Conf. Geotechnical Engineering*, 987-988 (in Japanese).
- Okamura, M., Takebayashi, M., Nishida, K., Fujii, N., Jinguji, M., Imasato, T., Yasuhara, H. & Nakagawa, E. 2011. In-situ desaturation test by air injection and its evaluation through field monitoring and multiphase flow simulation, *Journal of Geotechnical and Geoenvironmental Engineering*, ASCE, 137(7): 643-652.
- Orense, R.P., Morimoto, I., Yamamoto, Y., Yumiyama, T., Yamamoto, H. & Sugawara, K. 2003. Study on wall-type gravel drains as liquefaction countermeasure for underground structures, *Soil Dynamics and Earthquake Engineering* 23: 19-39.
- Otsubo, M., Towhata, I., Hayashida, T., Shimura, M., Uchimura, T., Liu, B., Taeseri, D., Cauvin, B. & Rattetz, H. 2016a. Shaking table tests on mitigation of liquefaction vulnerability for existing embedded lifelines, *Soils and Foundations*, 56(3): 348–364.
- Otsubo, M., Towhata, I., Hayashida, T., Liu, B. & Goto, S. 2016b. Shaking table tests on liquefaction mitigation of embedded lifelines by backfilling with recycled materials, *Soils and Foundations*, 56(3): 365-378.
- Plafker, G. 1969. Tectonics of the March 27, 1964, Alaska earthquake, USGS Professional Report “The Alaska Earthquake, March 27, 1964: Regional effects”, Report No. 543-I.
- Razouli, R., Towhata, I. & Akima, T. 2016. Experimental evaluation of drainage pipes as a mitigation against liquefaction-induced settlement of structures, *Journal of Geotechnical and Geoenvironmental Engineering*, ASCE, 142(9).
- Rikuzen-Takata City 2016. Reconstruction of Rikuzen-Takata (in Japanese).
- Sasaki, Y., Towhata, I., Miyamoto, K., Shirato, M., Narita, A., Sasaki, T. & Sako, S. 2012. Reconnaissance report on damage in and around river levees caused by the 2011 off the Pacific coast of Tohoku Earthquake, *Soils and Foundations*, 52(5): 1016-1032.

- Suwa, S. & M. Fukuda 2014. Case Study on Countermeasure to Liquefaction by Dewatering Method, *Journal of the Society of Materials Science, Japan*, 63(1): 21-27.
- Takahashi, H., Takahashi, N., Morikawa, Y., Towhata, I. & Takano, D. 2016. Efficacy of pile-type improvement against lateral flow of liquefied ground, *Geotechnique*, 66(8): 617-626.
- Tatsuoka, F., Iwasaki, T., Tokida, K., Yasuda, S., Hirose, M., Imai, T. & Kon-no, M. 1980. Standard penetration tests and soil liquefaction potential evaluation, *Soils and Foundations*, 20(4): 95-111.
- Tatsuoka, F., Kato, H., Kimura, M. & Pradhan, T.B.S. 1988. Liquefaction strength of sands subjected to sustained pressure. *Soils and Foundations – JGS* 28(1): 119-131.
- Tokimatsu, K. & Yoshimi, Y. 1983. Empirical correlation of soil liquefaction based on SPT N-value and fines content, *Soils and Foundations*, 23(4): 56-74.
- Tokimatsu, K. 1997. Earthquake resistant design for buildings and SPT-N value, *The Foundation Engineering & Equipment, Monthly*, 25 (12):61-66 (in Japanese).
- Tobita, T., Kang, G.C. & Iai, S. 2011. Centrifuge modeling on manhole uplift in a liquefied trench, *Soils and Foundations*, 51(6): 1091-1102.
- Towhata, I., Maruyama, S., Kasuda, K., Koseki, J., Wakamatsu, K., Kiku, H., Kiyota, T., Yasuda, S., Taguchi, Y., Aoyama, S. & Hayashida, T. 2014. Liquefaction in Kanto Region during the East-Japan gigantic earthquake on March 11, 2011, *Soils and Foundations*, 54(4): 859-873.
- Towhata, I., Morikawa, Y., Takahashi, H., Takahashi, N. & Sugawa, T. 2015a. Centrifuge model tests on mitigation against liquefied-soil lateral flow by using cement treated soil columns, 16th European Regional Conference on Soil Mechanics and Geotechnical Engineering, Edinburgh, 1199-1204.
- Towhata, I. & Nakamura, H. 2015b. Qualified evaluator of subsoil quality for safety of residential land, *Int. Conf. Soft Ground Engineering (ICSGE2015)*, Singapore, Paper No. 180.
- Towhata, I., Taguchi, Y., Hayashida, T., Goto, S., Shintaku, Y., Hamada, Y. & Aoyama, S. 2016a. Liquefaction perspective of soil ageing, *Geotechnique*, 67(6): 467-478.
- Towhata, I., Yasuda, S., Yoshida, K., Motohashi, A., Sato, S. & Arai, M. 2016b. Qualification of residential land from the viewpoint of liquefaction vulnerability, *Soil Dynamics and Earthquake Engineering Journal*, 91:260-271.
- Towhata, I. 2018. Progress of Liquefaction Ageing in Seismically Active Japan. *Proc. GEESDV Geotechnical Earthquake Engineering and Soil Dynamics V*, GeoInstitute of ASCE, Austin, Texas. GSP 290: 473-483.
- Towhata, I., Komine, H., Goto, S., Suzuki, M., Hishioka, S. & Watanabe, Y. 2018. Geotechnical engineering for nuclear decommission, *Journal of Nuclear Fuel Cycle and Environment, Atomic Energy Society of Japan, ATOMOS*, 25 (2):85-90 (in Japanese).
- Uda, T., San-nami, T., Hoshigami, Y. & Sakai, K. 2012. Damage due to the 2011 great tsunami and shrines escaped from being damaged, *Proc. JSCE B3 68 (2):I_43-I_48* (in Japanese).
- Yamazaki, K. 2013. Disaster and Shrine, *Proc. Annual Meeting of the Association of Japanese Geographers*, p. 100038 (in Japanese).
- Yasuda, S. & T. Hashimoto 2002. Subsidence of houses due to liquefaction during the 2000 Tottoriken Seibu earthquake, 57th Annual Conf. JSCE, Paper III-515: 1029-1030 (In Japanese).
- Yasuda S. 2004. Damage in residential district caused by Tottori-ken Seibu earthquake, *Journal of Comprehensive Papers, Architectural Institute of Japan*, 119(2):45-46.
- Yasuda, S., Sasaki, S., Noguchi, C. & Ozawa, N. 2013a. Shaking table tests to study the possibility to prevent liquefaction-induced damage of houses by installing sheet piles (Part 1), *Proc. 48th JGS National Conference*, 1759-1760 (in Japanese).
- Yasuda, S., Sasaki, S., Noguchi, C. & Ozawa, N. 2013b. Shaking table tests to study the possibility to prevent liquefaction-induced damage of houses by installing sheet piles (Part 2), 48th JGS National Conference, 1761-1762 (in Japanese).
- Yasuda, S. & Hashimoto, T. 2016. New project to prevent liquefaction-induced damage in a wide existing residential area by lowering the ground water table, *Soil Dynamics and Earthquake Engineering* 91: 246-259.
- Yoshida, M., Miyajima, M. & Kitaura, M. 2008. Experimental study on mitigation of liquefaction-induced floatation of sewerage manhole by using permeable recycled materials packed in sandbags. *Proc. 14th World Conference on Earthquake Engineering*. Beijing, China.
- Yoshikawa, E., Komine, H., Goto, S., Yoshimura, M., Suzuki, M., Narushima, S., Arai, Y., Ujiie, S., Sakoda, Y. & Nagae, Y. 2017. The quantitative evaluation for radiation shielding capabilities of soil materials. *Proc JSCE C*, 73(4): 342-354 (in Japanese).
- Wichtmann, T., Niemunis, A., Triantafyllidis, Th. & Poblete, M. 2005. Correlation of cyclic preloading with the liquefaction resistance, *Soil Dynamics and Earthquake Engineering*, 25: 923-932.